Remote Sensing of Environment 115 (2011) 343–352

Contents lists available at ScienceDirect

Remote Sensing of Environment

journal homepage: www.elsevier.com/locate/rse

Assessing drought probability for agricultural areas in Africa with coarse resolution remote sensing imagery

O. Rojas [a], A. Vrieling [b], F. Rembold [a,*]

[a] Joint Research Centre, European Commission, TP 266, 21027 Ispra (VA), Italy
[b] University of Twente, Faculty of Geo-Information Science and Earth Observation, P.O. Box 6, 7500 AA Enschede, The Netherlands

ARTICLE INFO

Article history:
Received 29 March 2010
Received in revised form 7 September 2010
Accepted 18 September 2010

Keywords:
Agricultural drought
Remote sensing
NDVI
Africa
Drought probability

ABSTRACT

Drought is one of the most frequent climate-related disasters occurring across large portions of the African continent, often with devastating consequences for the food security of agricultural households. This study proposes a novel method for calculating the empirical probability of having a significant proportion of the total agricultural area affected by drought at sub-national level. First, we used the per-pixel Vegetation Health Index (VHI) from the Advanced Very High Resolution Radiometer (AVHRR) averaged over the crop season as main drought indicator. A phenological model based on NDVI was employed for defining the start of season (SOS) and end of the grain filling stage (GFS) dates. Second, the per-pixel average VHI was aggregated for agricultural areas at sub-national level in order to obtain a drought intensity indicator. Seasonal VHI averaging according to the phenological model proved to be a valid drought indicator for the African continent, and is highly correlated with the drought events recorded during the period (1981–2009). The final results express the empirical probability of drought occurrence over both the temporal and the spatial domain, representing a promising tool for future drought monitoring.

1. Introduction

Droughts can have devastating effects on water supply, crop production, and rearing of livestock. They may lead to famine, malnutrition, epidemics and displacement of large populations from one area to another. The agricultural droughts across Africa of the 1980s and early 1990s have affected many countries and people and were probably some of the most shocking famine emergencies in recent history (Gommes & Petrassi, 1994). The International Disaster database of the Centre for Research on the Epidemiology of Disasters (CRED), reports more than 0.5 million deaths and 253 million people affected by drought events during the last 30 years (1981–2010) in Africa (EM-DAT, 2010). Table 1 summarizes the major droughts that occurred in the continent during the last three decades.

Identification of drought prone areas and estimation of the probability of drought occurrence are fundamental for the implementation of programmes that aim to increase food security. For risk management programmes and for efficient food-aid delivery, knowing the probability of drought occurrence is of basic importance. Furthermore, drought information at administrative levels is very important for a better interpretation of potential effects of climate change in Africa.

Drought risk calculation at continental scale is currently limited by the scarcity of reliable rainfall data. The coverage of operational weather stations in most African countries shows large spatial gaps and individual stations often provide discontinuous data. Due to those reasons, rainfall measurements are commonly replaced by data generated by atmospheric circulation models and/or satellite observations. Commonly used rainfall datasets for monitoring food security are the precipitation forecasts of the European Centre for Medium-Range Weather Forecast (ECMWF) and the rainfall estimates (RFE) produced by the Climate Prediction Centre (CPC) of the National Oceanic and Atmospheric Administration (NOAA). Several other sources exist, like for example the Tropical Rainfall Measuring Mission (TRMM), the Tropical Applications of Meteorology using SATellite (TAMSAT) products at Reading University, and the FAO rainfall estimates (http://geonetwork3.fao.org/climpag/FAO-RFE.php). However, all the mentioned rainfall estimates contain errors and show deviations in different regions of Africa (Dinku et al., 2007; Lim & Ho, 2000; Rojas et al., in press). At the same time, validation or better calibration of these rainfall estimates is hindered by the scarce availability of ground (rain gauge) measurements. This makes it extremely difficult to assess the quality or reliability of each dataset, which can have important implications for food security applications (Verdin et al., 2005).

On the other hand, vegetation abundance and development information, which is strongly related to rainfall, can also be used for drought assessment. Field studies and airborne scanner experiments (Tucker, 1979) demonstrated that the spectral reflectance properties of

* Corresponding author. Tel.: +39 0332 786337; fax: +39 0332 785162.
E-mail address: felix.rembold@jrc.ec.europa.eu (F. Rembold).

0034-4257/$ – see front matter © 2010 Elsevier Inc. All rights reserved.
doi:10.1016/j.rse.2010.09.006

Table 1
Major droughts ocurred in the African Continent during the period 1980–2010.

Region	1980–89	1990–99	2000–09
Northern Africa		In Morocco, agricultural output recorded losses in 1992, 1995 and 1997 due to drought. In 1997, Algeria's cereal harvest decreased sharply as a result of severe drought (UNEP, 2002).	The most recent drought in Tunisia and Algeria (from 1999-2002) appears to be the worst since the mid-15th century. That's according to researchers who recently analysed tree-ring records from the region (http://environmentalresearchweb.org/cws.article/news/35673).
West Africa	The Sahel was hit by a severe drought in the early-mid 1980's (Brooks, 2004). The worst drought in the Sahel during this period occurred during the year 1984 affecting most Sahel countries (Gommes & Petrassi, 1994).		
Eastern Africa	The lowlands of Ethiopia and the main productive areas of Kenya have been affected by the 1984 drought (Gommes & Petrassi, 1994). In Ethiopia, the 1984 drought caused the deaths of about 1 million people, 1.5 million head of livestock perished, and 8.7 million were affected in all. In 1987, more than 5.2 million people in Ethiopia, 1 million in Eritrea and 200 000 in Somalia were severely affected (Drought Monitoring Center, 2000).		Rainfall records indicate that, in some parts of the sub-region, the drought in 2000 was worse than that experienced in 1984 (Drought Monitoring Center, 2000).
Southern Africa	In 1982/83 much of Southern Africa was severely affected (Drought Monitoring Center, 2000).	Most of the Southern Africa countries were severely affected by the 1991/92 drought, which was the most severe after the 1982/83 drought (Gommes & Petrassi, 1994). The drought of 1991/92 was the severest on record, causing a 54% reduction in cereal harvest and exposing more than 17 million people to risk of starvation (Calliham et al., 1994; UNEP, 2002).	

vegetation canopies, and in particular combinations of the red and near infrared reflectance (so called "vegetation indices" or VI), are very useful for monitoring green vegetation. Among the different VIs based on these two spectral channels, is the NDVI (Normalized Difference Vegetation Index), proposed by Deering (1978), which is the most popular indicator for studying vegetation health and crop production (MacDonald & Hall, 1980; Sellers, 1985). Research in vegetation monitoring has shown that NDVI is closely related to the LAI (leaf area index) and to the photosynthetic activity of green vegetation. NDVI is an indirect measure of primary productivity through its quasi-linear relation with the fAPAR (Fraction of Absorbed Photosynthetically Active Radiation) (Los, 1998; Prince, 1990). NDVI is affected by some well known limitations as for example effects of soil humidity and surface anisotropy. Composite products used in most applications tend to limit these effects but they cannot be ignored completely. As a consequence NDVI values may slightly vary due to soil humidity and depending on the particular anisotropy of the target as well as on the angular geometry of illumination and observation at the time of the measurements. This is particularly relevant for AVHRR derived data since the orbit of the NOAA platforms tended to drift in time and the 25 years time series is composed by data from several different sensors (Tucker et al., 2005).

At present, several time series of satellite derived vegetation indices at the global scale and with a high temporal frequency are freely available. These include MODIS (Moderate Resolution Imaging Spectroradiometer), SPOT (Satellite Pour l'Observation de la Terre) VEGETATION, and AVHRR (Advanced Very High Resolution Radiometer). Although the spatial resolution is relatively low, AVHRR has the longest time series and also offers the advantage of a thermal channel. The AVHRR sensor was flown on different NOAA satellites since 1979. A large number of derived products exist, which continue to be updated until present. The main objective of this study is to evaluate the probability of agricultural drought occurrence for the African continent without depending on the scarcity and low quality of rainfall data sets. For that purpose we use vegetation indices derived from AVHRR data. Final probabilities are derived by aggregating results at the sub-national administrative level.

2. Materials and methods

2.1. Data

The main data used for this study are existing long term time series of NOAA AVHRR data. Two series made available by different research groups were combined in this work:

1) The Vegetation Health Index (VHI) produced by the Center for Satellite Applications and Research (STAR) of the National Environmental Satellite, Data and Information Service (NESDIS). This data set consists of weekly VHI images at 16 km resolution for the period 1981 (week 35)–2010 (week 11).[1] http://www.star.nesdis.noaa.gov/smcd/emb/vci/VH/vh_ftp.php
2) The Normalized Difference Vegetation Index (NDVI) dataset from the NASA Global Inventory Monitoring and Modeling Systems (GIMMS) Group at the Laboratory for Terrestrial Physics (Tucker et al., 2005). This dataset consists of 15-day maximum-value composites at 8 km resolution. We used the data from July 1981 to December 2006 for the African window. http://glcf.umd.edu/data/gimms/

Two additional spatial data sources were used for aggregating the VHI over space: a crop mask and administrative regions boundaries. The crop mask was constructed by using both the crop zones developed by FAO in the 90s, and the Global Land Cover (GLC2000) (Bartholomé & Belward, 2005). The administrative regions were obtained from the Global Administrative Unit Layers (GAUL) database. GAUL is an initiative implemented by FAO funded by the European Commission http://www.foodsec.org/tools_gaul.htm. It aims at providing the most reliable spatial information on administrative units for all the countries in the world. Here we used the first sub-national administrative units (level 1) in order to have a homogeneous reference layer at the continental scale. This implies

[1] From week 36 of 1994 to week 3 of 1995 data are not present due to sensor problems.

that according to the different political organizations of each country, the size of individual units is highly variable.

2.2. Methodology

2.2.1. Vegetation Health Index (VHI)

For drought assessment we selected the Vegetation Health Index (VHI) developed by Kogan (1995, 1997), who has successfully applied it for numerous case studies in many different environmental conditions around the globe, including Asia (Kogan et al., 2005; Ramesh et al., 2003), Africa (Unganai & Kogan, 1998) , Europe (Kogan, 1986), North America (Kogan, 1995; Salazar et al., 2007) and South America (Seiler et al., 2007). VHI is a composite index joining the Vegetation Condition Index (VCI) and the Temperature Condition Index (TCI).

The VCI (Kogan, 1994) is derived from the Normalized Difference Vegetation Index (NDVI). It is a scaling of the NDVI between its maximum and minimum value, and can be expressed as:

$$VCI_i = 100^*(NDVI_i - NDVI_{min}) / (NDVI_{max} - NDVI_{min}) \quad (1)$$

where $NDVI_i$ is the smoothed weekly NDVI, and $NDVI_{max}$ and $NDVI_{min}$ are absolute maximum and minimum NDVI, respectively, calculated for each pixel and week during the period 1981–2010 of the smoothed NDVI. VCI was designed to separate the weather related component of NDVI from ecological factors (Kogan, 1994). In general the VCI captures rainfall dynamics better than NDVI particularly in geographically heterogeneous areas. The VCI not only reflects the spatial and temporal vegetation variability but also allows quantifying the impact of weather on vegetation (Kogan, 1994; Unganai & Kogan, 1998).

The TCI algorithm is similar to VCI, but relates to the brightness temperature T estimated from the thermal infrared band of AVHRR (channel 4). Kogan (1995) proposed this index to remove the effects of cloud contamination in the satellite assessment of vegetation condition due to the fact that the AVHRR channel 4 is less sensitive to water vapor in the atmosphere compared with the visible light channels. High temperatures in the middle of the season indicate unfavorable or drought conditions while low temperature indicates mostly favorable conditions (Kogan, 1995). The expression consequently is:

$$TCI_i = 100^*(T_{max} - T_i) / (T_{max} - T_{min}) \quad (2)$$

VHI is expressed as:

$$VHI_i = w_1{}^*VCI_i + w_2{}^*TCI_i; \quad (3)$$

It is the additive combination of VCI and TCI for week i. In some studies different weights (w1 and w2) are assigned to VCI and TCI. For example, Unganai and Kogan (1998) determined the weights based on the correlation between VCI and TCI with corn yield anomalies. In near normal conditions, vegetation is more sensitive to moisture during canopy formation (leaf appearance) and to temperature during flowering. Since moisture and temperature contribution during the crop cycle is currently not known, we assume that the share of weekly VCI and TCI is equal ($w_1 = w_2 = 0.5$).

2.2.2. Agricultural crop mask

In order to assess agricultural drought we created an agricultural crop mask for the African continent, using the FAO GIEWS main crop zones and the GLC2000 land cover map. We first took the total extent of the FAO main crop zones for the following annual crops: pulses, sorghum, wheat, millet, teff, maize, niebe, yams, rice and barley. The zones are rather coarse and often overlapping. We therefore used the more detailed GLC2000 to refine the mask by excluding bare soils and forest. Instead of using directly the GLC2000 agricultural classes we preferred an exclusion approach. The main reason for this is that the GLC2000 forest and bare soil classes have shown a higher accuracy than the agricultural classes (Mayaux et al., 2004).The combination of the described steps resulted in a single crop mask for Africa.

2.2.3. Determination of the optimal VHI integration period for agricultural areas (temporal aggregation)

VHI can detect drought conditions at any time of the year. For agriculture, however, we are only interested in the period most sensitive for crop growth (vegetative stage, flowering and grain filling) (Doorenbos & Kassam, 1979). In this study we decided to use the same period (i.e. weeks) for all pixels within individual administrative units. Moreover, we do not shift this period between different years.

To determine the most sensitive period we first derived the start of season (SOS) and end of season (EOS) from the GIMMS NDVI time series. For this we used the 50%-threshold method of White et al. (1997) and implemented it in the same way as Vrieling et al. (2008). In short, for each pixel we first determine per year the maximum NDVI value and the preceding minimum NDVI value. SOS is the moment between maximum and minimum when NDVI reaches the average between maximum and minimum (i.e. 50% threshold). EOS is the moment after maximum when the NDVI-curve again reaches the same level (Fig. 1). For consistency in the multi-year analysis and within administrative units, the SOS and EOS-values were averaged for all years and all pixels within a unit. A double season was only retained for those units where at least 50% of the pixels allow for a good separation between two seasons (i.e. two clear minima and maxima).

A modification was done subsequently to the EOS (Fig. 1). The developmental stages at which crop plants are more sensitive to water deficit are the vegetative stage, the flowering and the grain filling (Doorenbos & Kassam, 1979). Restrictive water supply during these stages may affect productivity more severely than during other periods (establishment or ripening). The retrieved SOS generally coincides with the start of the crop development stage, approximately 25–30 days after crop planting according to our knowledge of African agriculture. This fact is due to the seasonal lag of NDVI response with respect to rainfall and varies for vegetation type in tropical Africa, i.e. 1–3 weeks in Equatorial rainforest, 2–6 weeks in the wet savanna and about 6–9 weeks in the dry savanna (Shinoda, 1995). Traditional rainfed farmers in Africa generally use the onset of the rainy season for crop planting. Normal planting time in Southern Africa is October–November, in the Sahel June–July, and in Eastern Africa, where double seasons are found, February–June. For EOS, the modeled values include the ripening stage that is less sensitive to water stress. To

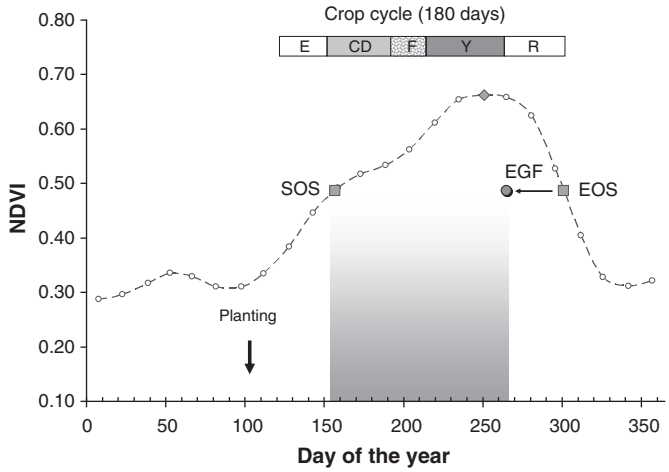

Fig. 1. Sample NDVI profile showing the period of analysis defined by the start of the season (SOS) and the end of the grain filling stage (EGF). The EGF is defined by the end of the season (EOS) minus 6 weeks (42 days). The crop cycle is divided into 5 development stages: E: establishment, CD: crop development, F: flowering, Y: yield formation or grain filling and R: ripening stage. Where CD, F and Y are the most sensitive to water deficit.

adjust the period of analysis to the most sensitive water stress stages of the crop, we subtracted 6 weeks from EOS. In this way we identify an end date at the end of the yield formation or grain filling stage instead of using the harvesting time (EGF = EOS − 6 weeks) (Fig. 1).

For each pixel and individual year, the weekly VHI values between the mean SOS and EGF were averaged to obtain a representative value of VHI for the drought-sensitive part of the crop season (temporal aggregation). This method takes into account the cumulative development of drought over a period of time. At pixel level the VHI average was only calculated if at least 75% of the crop season values were present. Otherwise, the pixel was treated as "missing data". In practice the only pixels with missing data are those in seasons with incomplete VHI data (1981/82 and 1994/95).

2.2.4. Geographic VHI aggregation

The temporal VHI aggregation was first carried out at pixel level (16 × 16 km) to identify drought prone areas across the whole African continent. In a second stage, in order to directly identify the administrative units affected by agricultural drought, we determined which percentage of the unit's agricultural area experienced VHI values below 35 during the crop season. This threshold was introduced by Kogan (1995) to identify drought conditions. He obtained this threshold correlating the VCI with different crop yields and diverse ecological conditions and found a logarithmic fit between VCI and crop yield with an r-square of 0.79.

Within each administrative unit, the analysis was limited to agricultural areas based on the crop mask described in Section 2.2.2. Only pixels covered at least for 25% by the crop mask were considered. A weighted average (with weights based on percentage covered by crop mask) was calculated for each administrative region. Regions were excluded in case less than 10 valid pixels were present, i.e. pixels having both a valid average VHI value and are covered for at least 25% by agriculture (Genovese et al., 2001).

The final results were aggregated at sub-national administrative level because this allows easy comparison with existing agricultural production statistics. For some countries (like Burundi, Rwanda, and Uganda) the administrative units are rather small and comprise a limited number of pixels, thus sometimes not allowing for effective VHI aggregation. In these cases however, we preferred to apply the existing administrative borders instead of creating artificial units. The results of the temporal and spatial VHI aggregation are 29 (1981–2009) annual maps showing the percentage of agricultural area affected by drought for each administrative unit.

2.2.5. Probability mapping

In order to compute the probability of drought affecting significant portions of the agricultural area of each administrative unit, we

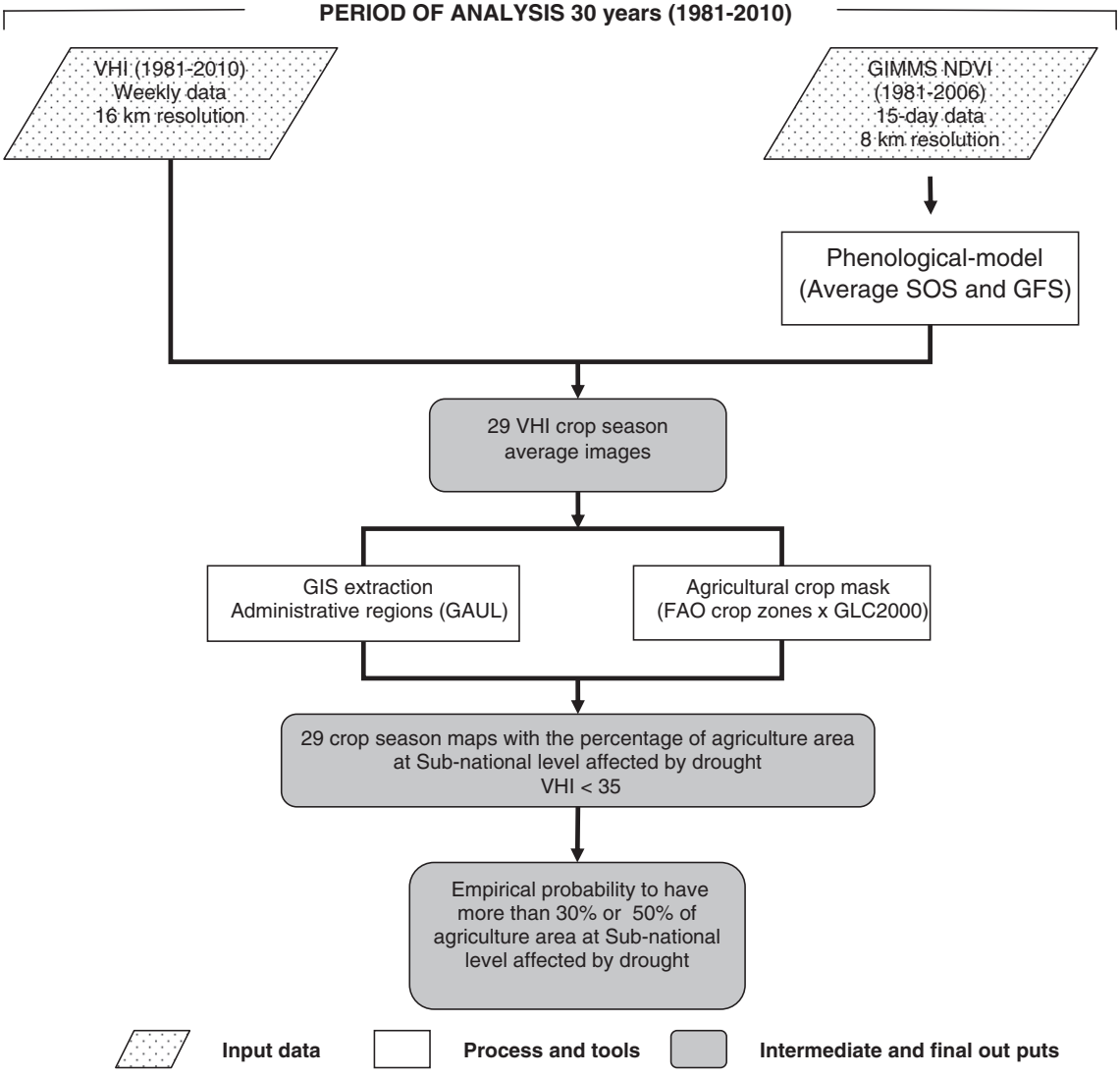

Fig. 2. Methodological flow-chart.

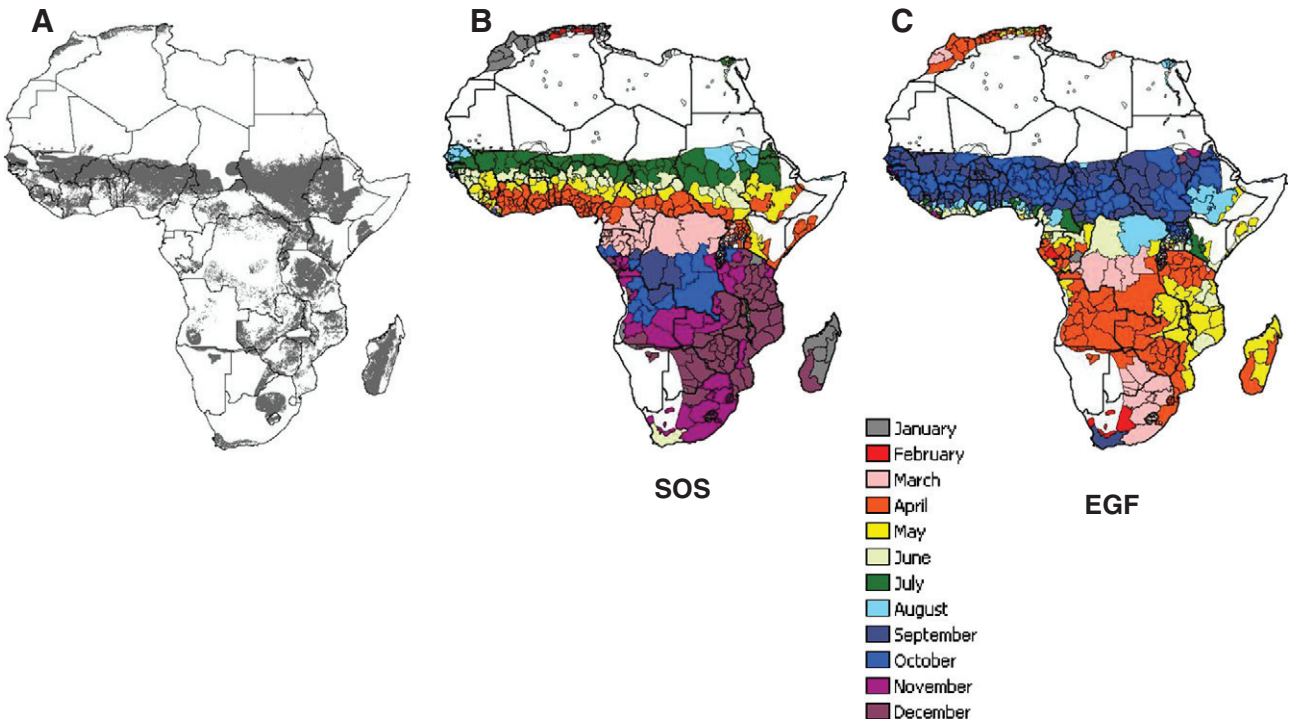

Fig. 3. (A) Agricultural crop mask considering the main FAO crop zones and masking out the forest using GLC2000 for the following annual crops: pulses, sorghum, wheat, millet, maize, niebe, teff, yams, rice and barley. (B) The start of crop development stage by administrative unit (C) end of the grain filling stage by administrative unit. In maps B and C a monthly color scale was used only for graphic representation, operationally a weekly time step is used.

introduced two minimum arbitrary thresholds, one of 30% and another of 50%. In practice, when over 30% of the total agricultural area of an administrative unit is affected by drought, we assume that a large number of agriculture households experience its consequences. When more than 50% of agricultural area is affected by drought, we can assume to be confronted with an extreme drought event with

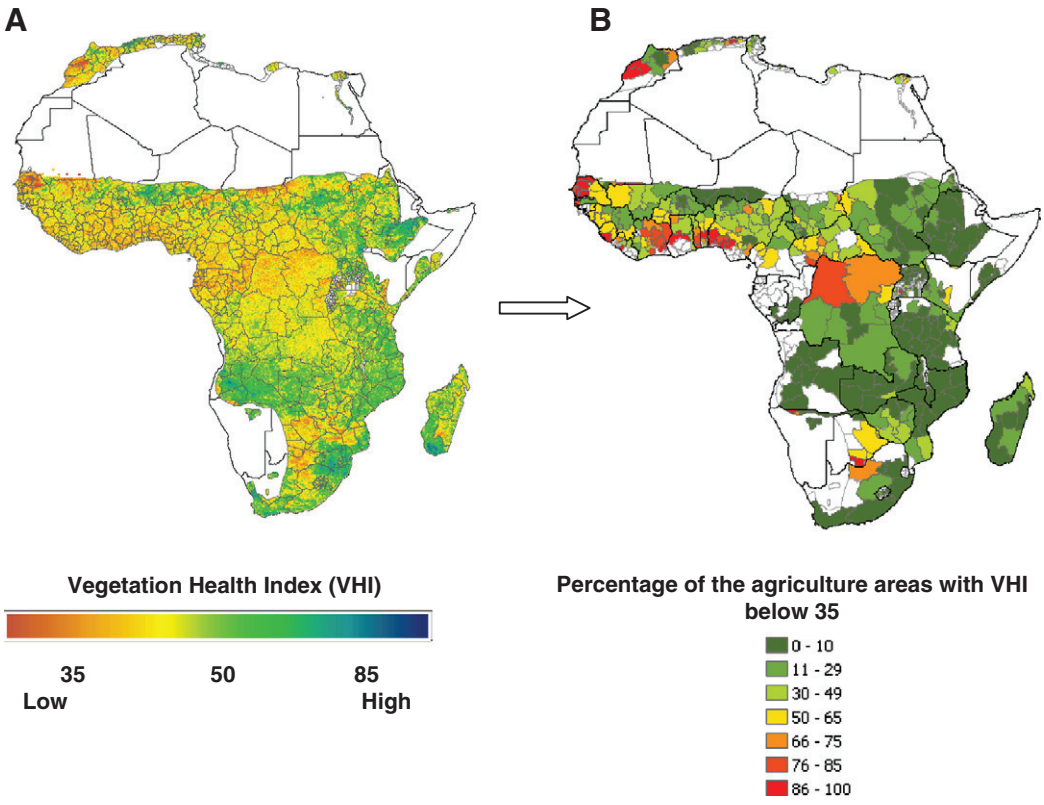

Fig. 4. (A) Average VHI image for the crop season 1983/84 (B) percentage of agricultural area affected by drought (VHI<35) based on (A). The average crop season VHI shows the temporal impact of drought while the percentage of affected agricultural area explains the spatial dimension of the drought.

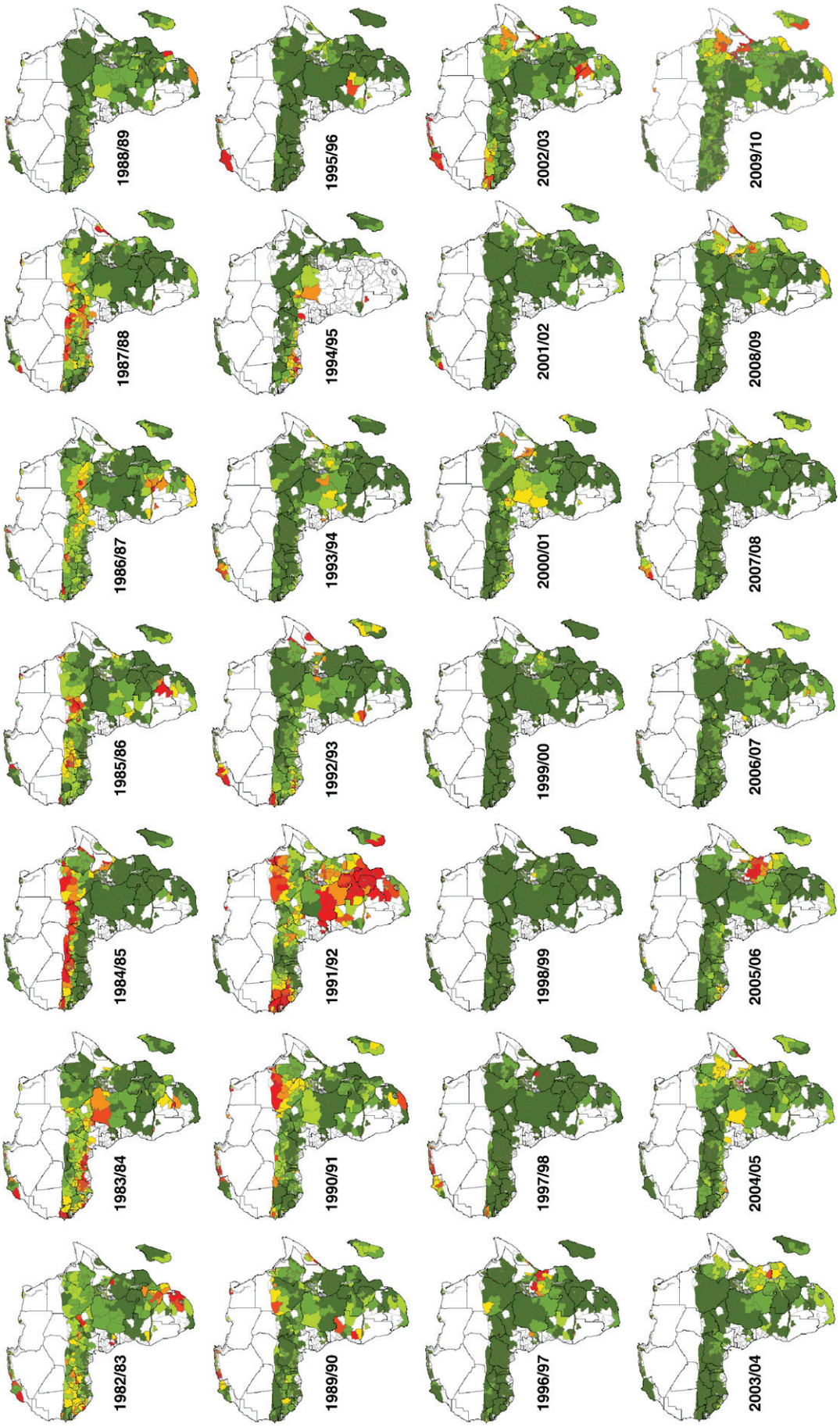

Fig. 5. Percentage of agricultural area affected by drought during the first crop season (VHI<35) from 1982 to 2010 (seasons 1994/95 and 2009/10 are incomplete).

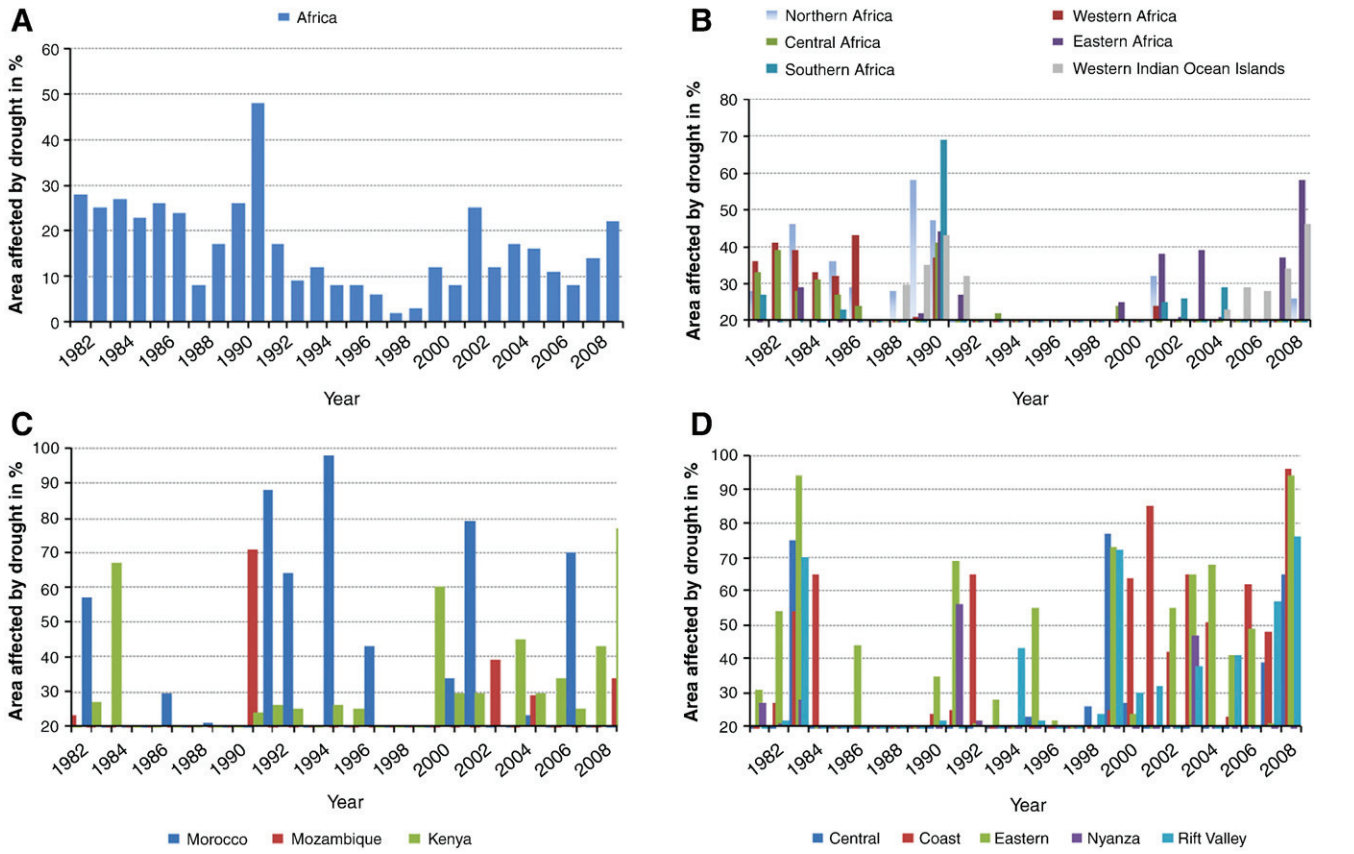

Fig. 6. Area affected by drought (VHI<35) at different scales of analysis: (A) Continental: the major drought occurred in 1991 (48% of agricultural area affected) followed by the 1982 drought (28%). (B) Regional: Western Africa affected from 1982 to 1998; all regions seriously affected by the drought in 1991 and Eastern Africa most affected during the 2000s. (C) National: Comparison of area affected in three countries: Morocco, Mozambique and Kenya. (D) Sub-national: Comparison of area affected by drought at the sub-national level in Kenya.

serious impact on regional food security. We assume that the occurrence of a certain percentage of area affected by drought in year "t" is independent on climate in other years. If P is the probability of a drought event, the number n of years that the event happens in a period of N years follows a binomial distribution (Evans et al., 2000); P is estimated by $\hat{P}=n/N$ and a confidence interval for P is: (Stuart & Ord, 1991; von Storch & Zwiers, 1999)

$$P \in \hat{P} \pm 2\sqrt{\hat{P}\left(1-\hat{P}/N\right.} \quad (4)$$

Fig. 2 summarizes the data analysis steps in a methodological flow-chart.

3. Results

3.1. Crop mask, SOS and EGF

Fig. 3 shows (A) the crop mask developed for this study; (B) the start of the crop development stage (that coincides with the start of the season of the phenological model, SOS) and (C) the end of the grain filling stage. In general the phenological model better reflects crop phenology of the relatively homogeneous crop areas in places with a short rainy season like the Sahel, than of the more complex crop associations in areas with a longer rainy season such as Eastern (Ethiopia and Southern Sudan) and Southern Africa (Mozambique and Madagascar). On the other hand, the phenological model detected the climate pattern differences in South Africa between the Western Cape crops (wheat and barley), which are cultivated from May to November and the crops in the Eastern part of South Africa (e.g. maize, sorghum, millet…) which grow from October to May. Both SOS and EGF have also been calculated for areas that have a clearly defined second crop season (Eastern Africa and some countries in the Guinea Gulf).

3.2. Average VHI for the crop season and percentage of agriculture area affected by drought

Fig. 4 shows an example of the transformation of VHI averaged during the crop season 1983/1984 at pixel level into the percentage of agricultural areas affected by drought (VHI below 35) at sub-national level. Averaging the VHI during the crop season shows the drought persistence during the cropping season. In addition, by calculating the percentage of drought-affected agricultural area, we analyzed the spatial impact of the drought at sub-national level for each crop season during the study period. The temporal and spatial aggregations give a good estimate of the drought intensity during the most water stress sensitive stages for crops. Fig. 5 presents the percentage of agricultural area affected by drought for each crop season from 1982/83 to 2009/10. All the major drought events suffered by the African continent and reported in Table 1 can easily be identified at different geographic scales in Figs. 5 and 6. For example the droughts that hit the Sahel during the 1980s are clearly observable, and the worst drought that occurred during the year 1984 was well indentified (Gommes & Petrassi, 1994). This drought affected most Sahel countries, as well as the lowlands of Ethiopia and the main maize productive areas of Kenya. It was one of the most extensive droughts in the Sahel which reached well into Eastern Africa. Another impressive drought well detected by the proposed methodology occurred in Southern Africa during the cropping season 1991/92. Gommes and Petrassi (1994) mention that most of the Southern

Africa countries were severely affected by the 1991/92 drought, which was the most severe after the 1982/83 event, the latter having been the worst since the 1920s. Other examples of detected events relate to several North African countries which experienced serious drought events during the 90s such as Morocco (1992, 1995 and 1997) and Algeria (1997). For the analyzed period (1981–2009) the 1991/92 drought is clearly the largest drought that the Africa continent has suffered, affecting Southern Africa, part of Western Africa, and part of Eastern Africa (Fig. 5).

Fig. 6 shows the percentage of area affected by drought using different scales of analysis: continental, regional (we use the regions proposed by the Africa Environment Outlook http://www.unep.org/dewa/Africa/publications/aeo-1/009.htm), national (Morocco, Mozambique and Kenya) and sub-national (Kenya). The analysis done at different scales proves the flexibility of the methodological approach proposed in this paper, allowing international institutions interested in drought monitoring an easier understanding of the relative importance of local droughts. Knowing the extension and intensity of a drought a continental scale could facilitate the targeting of donor resources among drought-affected countries in Africa. In a country level the method provides a way of quickly assessing the magnitude of the current drought as compared with historical records (as can be seen for example in Fig. 6C, 1995 was clearly the worst drought in Morocco over the last 30 years). Finally, the sub-national level analysis shows the impact of localized drought on the national production and helps planning food-aid intervention measures by integration with other socioeconomic factors (population, livelihood, etc.) for the region affected.

3.3. Empirical probabilities at sub-national level

Fig. 7 shows the probabilities of exceeding the thresholds of 30% and 50% of the total agricultural area affected by drought. These thresholds can be modified depending on the objective of the study. For instance in an agricultural insurance scheme when fixing the insurance premium, the area affected could be correlated with the anticipated economic losses following the drought. For food security projects, the thresholds could be related with the number of people affected and the number of rations needed to overcome the food-gap.

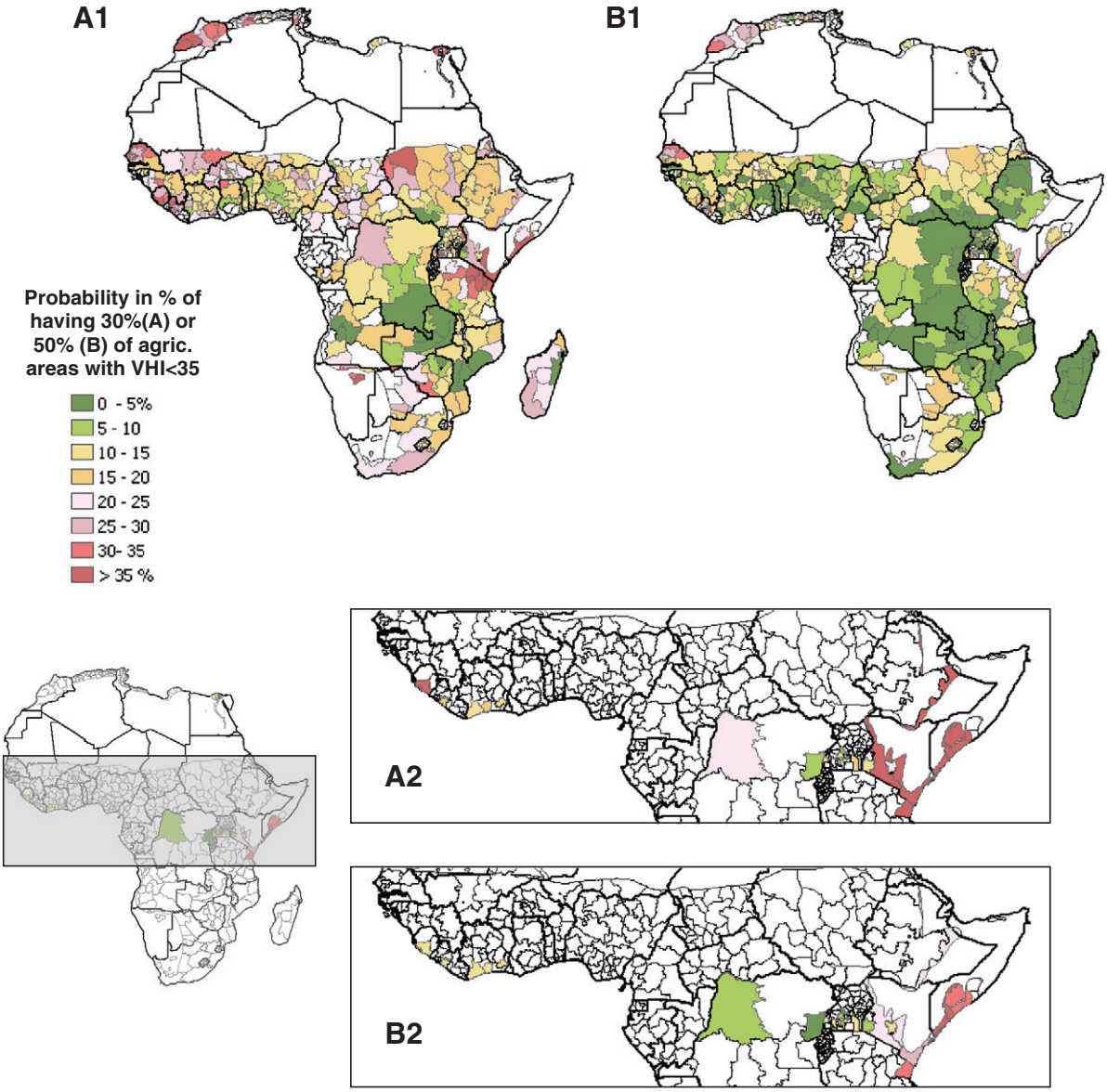

Fig. 7. Probability of occurrence of having more than 30% (A) or more than 50 % (B) of the agricultural area affected by drought by administrative unit (1) during the first crop season (2) during the second crop season.

Extreme agrometeorological events are at the same time rare (low statistical frequency) and characterized by high intensity (Gommes, 1999). The extended droughts of 1984 and 1991/92 that occurred in the Sahel and Southern Africa, were exceptional because they were intense and involved large clusters of administrative units at the same time, representing extraordinary events at the continental level. However the situation changes when the analysis is focused on the agricultural area affected by drought at sub-national level because from this perspective, all droughts are relevant and important. For instance several local "hot spots" were identified with empirical probabilities above 35% (3.5 times every 10 years) to have at least 30% of agriculture affected (Fig. 7-A1): Tensift and Centre in Morroco, Brakna in Mauritania, North Darfur in Sudan, Semenawi Keih Bahri in Eritrea, Coast and Eastern in Kenya, Manyara, Tanga, Arusha and Kilimanjaro in Tanzania, Juba Hoose, Juba Dhexe and Shabelle Hoose in Somalia, Kaabong and Kiruhura in Uganda, Southern in Sierra Leone, Gbarpolu in Liberia and Otjozondjupa in Namibia.

4. Discussion and conclusions

In general the developed methodology proved useful to identify major historical droughts over the observed period (1981–2009), as well as for identifying the impact of these events on agricultural areas over the whole African continent. Furthermore it was possible to geographically identify the administrative areas exposed to high risk of drought. These results should be analyzed considering socioeconomic factors, such as population increase and livelihood strategies, to have a more comprehensive assessment of the vulnerability of local populations to these droughts. For instance, the rapid population growth in Africa, which has placed extreme pressure on scarce land resources, and a lack of access to the assets is increasing the vulnerability of many regions to drought. In these areas, where smallholder livelihoods are undiversified and are dominated by subsistence-oriented food crop production, even a moderate drought that will cause a decline in harvests can be devastating for household food security.

It is also evident that per-pixel analysis of drought indicators is only useful for the detection of major (historical) droughts if the temporal integration is coupled with spatial aggregation. In this case we looked specifically at agricultural drought, but depending on the drought impact on other land use categories (forest, pastoralist areas, protected areas, etc.) the same methodological approach could be applied with minor adaptations.

The results shown in Figs. 5 and 7, provide a powerful tool for early warning and agricultural monitoring systems to quickly identify drought-sensitive areas at a continental or regional level, and to refine the analysis locally by analyzing drought indicators at pixel level or using more precise local data. Rainfall-based indices can be used for these areas if good quality records are available, otherwise the drought probability maps could be helpful in identifying new locations for rainfall stations for drought monitoring. For early warning and agricultural monitoring the proposed methodological approach could be adjusted to be run on a continuous basis. The SOS date could be calculated in real time (varying from year to year) and the VHI would be averaged weekly until reaching the EGF date. Every week during the crop season the percentage of area affected by drought could be calculated. In this way, the percentage of area affected by drought (e.g. 30%) could be linked to a temporal condition in order to establish the best date for issuing a drought warning (i.e. when at least 50% of the length of the crop cycle is reached). As a confirmation of this approach it can be observed that the results of the first crop season 2009/10 for East Africa, are in line with the drought warnings included in several early warning reports for the same area (Famine Early Warning System (FEWS-NET) http://www.fews.net/docs/Publications/kenya_09_2009_final.pdf, Monitoring Agricultural ResourceS (MARS), http://mars.jrc.ec.europa.eu/mars/content/download/1452/8205/file/EA_Kenya_July_2009.pdf).

For the areas with a second crop season, the second season generally shows a higher probability to suffer from drought. In East Africa this is in line with the fact that the second crop season (approx. October-January) is normally the shorter one, corresponding to shorter and more erratic rainfall than during the first crop season (approx. April–September).

The method presented in this study could be used in a more detailed way by looking at specific areas or countries and using detailed information on annual crop cycles instead of modeling the average crop cycle. At regional or country level, instead of GAUL level 1 aggregation, the pixel level product (Fig. 4A) could be used as such or aggregated by any other administrative or thematic zoning used for food security monitoring.

Finally, climate change is likely to increase the risk of droughts in many parts of the continent, with declining and more erratic rainfall resulting in lower aggregate production and more unpredictable harvests in Africa (Boko et al., 2007). The final drought probability represents a preliminary input for more detailed climate change analysis and prediction. The areas with high drought probability should be closely monitored and should have special contingency plans to reduce drought impact. Although in this study some geographic dynamics of drought events is apparent, i.e. concentrated in the Sahel during the 80s and in Southern Africa during the 90s, the period of analysis is too short to relate this to climate change.

Acknowledgements

The authors would like to thank Javier Gallego (JRC), Rene Gommes (FAO), Olivier Leo (JRC) and Simon Kay (JRC) for the useful suggestions and comments.

References

Bartholomé, E., & Belward, A. S. (2005). GLC2000: A new approach to global land cover mapping from earth observation data. *International Journal of Remote Sensing*, *26*(9), 1959−1977.

Boko, M., Niang, I., Nyong, A., Vogel, C., Githeko, A., Medany, M., et al. (2007). Africa. In M. L. Parry, O. F. Canziani, J. P. Palutikof, P. J. van der Linden, & C. E. Hanson (Eds.), *Climate change 2007: Impacts, adaptation and vulnerability. Contribution of Working Group II to the Fourth Assessment Report of the Intergovernmental Panel on Climate Change* (pp. 433−467). Cambridge UK: Cambridge University Press.

Brooks, N. (2004). *Drought in the African Sahel: long term perspectives and future prospects. Tyndall Centre for Climate Change Research*. University of East Anglia. Working paper.

Calliham, D. M., Eriksen, J. H., & Herrick, A. B. (1994). *Famine averted: The United States government response to the 1991/92 Southern Africa drought.* Evaluation Synthesis Report. Washington: Management Systems International.

Deering, D. W. (1978). Rangeland reflectance characteristics measured by aircraft and spacecraft sensors. Ph.D. Dissertation, Texas A&M University, College Station, TX, 388 pp.

Dinku, T., Ceccato, P., Grover-Kopec, E., Lemma, M., Connor, S. J., & Ropelewski, C. F. (2007). Validation of satellite rainfall products over East Africa's complex topography. *International Journal of Remote Sensing.*, *28*(7), 1503−1526.

Doorenbos, J., & Kassam, A. (1979). *Yield response to water.*FAO Irrigation and Drainage Paper No. 33. Rome: FAO 200 pp.

Drought Monitoring Centre (2000). Dekad 19 report (1–10 July, 2000) Ten day bulletin. *No. DMCN/01/337/19/07/2000. Drought Monitoring Centre, Nairobi, Kenya.*

EM-DAT (2010). *The OFDA/CRED International Disaster Database—www.emdat.net—Université Catholique de Louvain–Brussels–Belgium.*

Evans, M., Hastings, N., & Peacock, B. (2000). *Statistical distributions*, 3rd ed. New York: John Wiley and Sons (Chapter 6).

Genovese, G., Vignolles, C., Nègre, T., & Passera, G. (2001). A methodology for a combined use of normalized difference vegetation index and CORINE land cover data for crop yield monitoring and forecasting. A case study on Spain. *Agronomie*, *21*(1), 91−111.

Gommes, R. (1999). Extreme agrometeorological events, Discussion leading to the terms of reference for a database. *WMO CagM-12 WG on extreme agrometeorological events* 17 pp.

Gommes, R., & Petrassi, F. (1994). Rainfall variability and drought in sub-Saharan Africa since 1960. *FAO Agrometeorology Series Working Papers No. 9* 100 pp.

Kogan, F. (1986). *The impact of climate and technology on Soviet grain production.*: Delphic Association Rep. 174 pp.

Kogan, F. (1994). Droughts of the late 1980's in the United States as derived from NOAA polar-orbiting satellite data. *Bulletin of the American Meteorological Society*, *76*(5), 655−668.

Kogan, F. (1995). Application of vegetation index and brightness temperature for drought detection. *Advances in Space Research*, *15*, 91−100.

Kogan, F. (1997). Global drought watch from space. *Bulletin of the American Meteorological Society*, *7*(4), 621−636.
Kogan, F., Yang, B., Guo, W., Pei, Z., & Jiao, X. (2005). Modelling corn production in China using AVHRR-based vegetation health indices. *International Journal of Remote Sensing*, *26*(11), 2325−2336.
Lim, H. S., & Ho, C. H. (2000). Comparison of tropical rainfall between the observed GPCP data and the assimilation products of ECMWF, NCEP/NCAR, and NASA-GEOS-1. *Journal of the Meteorological Society of Japan*, *78*(5), 661−672.
Los, S. O. (1998). Linkages between global vegetation and climate. An analysis based on NOAA Advanced Very High Resolution Radiometer data. Ph.D. dissertation, Vrije Universiteit, Goddard Space Flight Centre, Greenbelt Maryland.
MacDonald, R. B., & Hall, F. G. (1980). Global crop forecasting. *Science*, *208*(4445), 670−679.
Mayaux, P., Bartholomé, E., Fritz, S., & Belward, A. (2004). A new land-cover map of Africa for the year 2000. *Journal of Biogeography*, *31*, 861−877.
Prince, S. D. (1990). High temporal frequency remote sensing of primary production using NOAA AVHRR. *Applications of remote sensing in agriculture*, *4*, 169−183.
Ramesh, P. S., Sudipa, R., & Kogan, F. (2003). Vegetation and temperature condition indices from NOAA AVHRR data for drought monitoring over India. *International Journal of Remote Sensing*, *24*(22), 4393−4402.
Rojas, O., Rembold, F., Delince, J., & Leo, O. (in press). Using NDVI as auxiliary data for rapid quality assessment of rainfall estimates in Africa. *International Journal of Remote Sensing*. doi:10.1080/01431161003698260.
Salazar, L., Kogan, F., & Roytman, L. (2007). Use of remote sensing data for estimation of winter wheat yield in the United States. *International Journal of Remote Sensing*, *28*(17), 3795−3811.
Seiler, R. A., Kogan, F., Guo, W., & Vinocur, M. (2007). Seasonal and interannual responses of the vegetation and production of crops in Cordoba, Argentina assessed by AVHRR-derived vegetation indices. *Advances in Space Research*, *39*(1), 88−94.
Sellers, P. J. (1985). Canopy reflectance, photosynthesis and transpiration. *International Journal of Remote Sensing*, *6*(8), 1335−1372.
Shinoda, M. (1995). Seasonal phase lag between rainfall and vegetation activity in tropical Africa as revealed by NOAA satellite data. *International Journal of Climatology*, *15*(6), 639−656, doi:10.1002/joc.3370150605.
Stuart, A., & Ord, K. (1991). *Kendall's advanced theory of statistics*.London: Griffin (Chapter 20).
Tucker, C. J. (1979). Red and photographic infrared linear combinations for monitoring vegetation. *Remote Sensing of Environment*, *8*, 127−150.
Tucker, C. J., Pinzón, J. E., Brown, M. E., Slayback, D. A., Pak, E. W., Mahoney, R., et al. (2005). An extended AVHRR 8 km NDVI dataset compatible with MODIS and SPOT vegetation NDVI data. *International Journal of Remote Sensing*, *26*(20), 4485−4498.
Unganai, L., & Kogan, F. (1998). Drought monitoring and corn yield estimation in Southern Africa from AVHRR data. *Remote Sensing of Environment*, *63*, 219−232.
United Nations Environmental Programme (2002). Africa environment outlook. *Past, present and future perspectives. Published to web by GRID-Arendal in 2002* Nairobi, Kenya. (ISBN 92-807-2101-1) 422 pp: UNEP.
Verdin, J., Funk, C., Senay, G., & Choularton, R. (2005). Climate science and famine early warning. *Philosophical Transactions of the Royal Society*, *360*, 2155−2168.
Von Storch, H., & Zwiers, F. W. (1999). *Statistical analysis in climate research*.Cambridge: University Press (ISBN 0 521 45071 3), 484 pp.
Vrieling, A., de Beurs, K. M., & Brown, M. E. (2008). Recent trends in agricultural production of Africa based on AVHRR NDVI time series. *Proceedings of SPIE, 7104, art. no. 71040R*.
White, M. A., Thornton, P. E., & Running, S. W. (1997). A continental phenology model for monitoring vegetation responses to inter-annual climatic variability. *Global Biogeochemical Cycles*, *11*(2), 217−234.